The Impact of Inter-flood Duration on Non-Cohesive Sediment Bed Stability

Annie Ockelford[1*], Stephen Woodcock[2], Heather Haynes[3]

1. *Centre for Aquatic Environments, University of Brighton, Brighton, BN2 4GJ* Email (a.ockelford@brighton.ac.uk) * corresponding author

2. *School of Mathematical Sciences University of Technology Sydney, Sydney, Australia NSW 2007*

3. *Water Academy, Heriot-Watt University, Edinburgh, EH14 4 AS*

Short Title: Inter- flood duration and bed stability

ABSTRACT

Limited field and flume data suggests that both uniform and graded beds appear to progressively stabilise when subjected to inter flood flows as characterised by the absence of active bedload transport. Previous work has shown that the degree of bed stabilization scales with duration of inter-flood flow, however, the sensitivity of this response to bed surface grain size distribution has not been explored. This paper presents the first detailed comparison of the dependence of graded bed stability on inter-flood flow duration. Sixty discrete experiments, including repetitions, were undertaken using three grain size distributions of identical D_{50} (4.8mm); near-uniform (σ_g = 1.13), unimodal (σ_g = 1.63) and bimodal (σ_g = 2.08). Each bed was conditioned for between 0 (benchmark) and 960 minutes by an antecedent shear stress below the entrainment threshold of the bed (τ^*_{c50}). The degree of bed stabilisation was determined by measuring changes to critical entrainment thresholds and bedload flux characteristics.

Results show that (i) increasing inter-flood duration from 0 to 960 minutes increases the average threshold shear stress of the D_{50} by up to 18%; (ii) bedload transport rates were reduced by up to 90% as inter-flood duration increased from 0 to 960 minutes; (iii) the rate of response to changes in inter-flood duration in both critical shear stress and bedload transport rate is nonlinear and is inversely proportional to antecedent duration; (iv) there is a grade dependent response to changes in critical shear stress where the magnitude of response in uniform beds is up to twice that of the graded beds; and (v) there is a grade dependent response to changes in bedload transport rate where the bimodal bed is most responsive in terms of the magnitude of change. These advances underpin the development of more accurate predictions of both entrainment thresholds and bedload flux timing and magnitude, as well as having implications for the management of environmental flow design.

Key Words; inter-flood duration, entrainment threshold, bedload flux, grain size distribution

1. INTRODUCTION

In non-cohesive sediment beds it is traditionally assumed that bed structure and hence, resistance to entrainment, is only capable of being modified when the applied shear stress exceeds the threshold for incipient motion (Gomez, 1983; Reid *et al.,* 1985; Church *et al*., 1998; Powell *et al.,* 1999). This theory suggests that low, inter-flood flow periods will have no effect on bed stability and bed restructuring will only occur during flood events which result in active bedload transport modifying surface stability. However, field (Reid and Frostick, 1984; Reid *et al.,* 1985; Masteller et al., 2019) and flume (Paphitis and Collins, 2005; Monteith and Pender, 2005; Haynes and Pender, 2007; Ockelford and Haynes, 2012; Masteller and Finnegan, 2017) data suggests that both uniform and graded beds appear to progressively stabilise even when subjected to the low shear stresses experienced during inter- flood flow periods.

Given that most commonly used sediment transport formulae use empirical relationships between bedload transport rate and flow intensity (Meyer-Peter & Müller, 1948; Bagnold, 1980; Ashmore, 1988; Parker, 1990; Zhang and McConnachie, 1994; Hassan and Woodsmith, 2004; Barry et al., 2008; Recking, 2010), and tend to rely on the assumption that a single critical value of shear stress can be used to predict the onset of motion (e.g., Meyer-Peter and Müller, 1948; Engelund and Fredsøe 1975; Wong and Parker, 2006) small errors in shear stress estimations can cause significant errors in bedload transport rate estimations (Buffington and Montgomery, 1997; Recking et al., 2012; Schneider et al., 2015). Thus, understanding how periods of prolonged, inter-flood flow, affect the onset of motion could be used to improve the predictive capability of certain sediment transport formulae.

These periods of antecedent flow have been termed ‘stress history’, which describes a time-dependent ‘memory’ effect, where the combined effect of the duration and magnitude of antecedent flows influences entrainment thresholds and bedload flux. This typically describes the low flow period between significant sediment-transporting events, where sediment transport rates are negligible or of very low exhibit low partial-transport conditions. Field data from the non-cohesive graded river bed of Turkey Brook showed entrainment thresholds up to three times higher during isolated flood events compared to floods which occurred with a shorter return period. Although not specifically quantified, it was hypothesised that shorter inter-flood durations left the bed material comparatively loose and more susceptible to entrainment in the subsequent flood event. As inter-flood duration increased more advanced bed re-structuring left the bed more resistant to entrainment with lower bedload transport rates in the subsequent flood (Reid and Frostick, 1984; Reid *et al.,* 1985). Pfeiffer and Finnegan (2018) observed that regional trends linked with hydrological regime controlled the bed surface mobility discussed in terms of the proportion of time a channel is above the conditions of threshold mobility; rivers characterised as having longer periods of high flow during snowmelt periods have higher relative mobility as compared to those characterised by abrupt brief flood events with longer inter- flood durations.

Direct laboratory evidence provides support for the importance of stress history effects. Paphitis and Collins (2005) studied the entrainment threshold for uniform sand beds subjected to antecedent flow durations of up to 120 minutes. Their data indicated the critical shear stress increased by up to 61% following exposure to prolonged durations of antecedent flow. Similarly, Monteith and Pender (2005) and Haynes and Pender (2007) exposed a bimodal sand-gravel mixture to increasing antecedent conditioning flow durations; up to a 48% increase in critical bed shear stress was noted as antecedent duration was increased from 0 to 5760 minutes. Bedload flux has also been shown to be responsive to the duration of antecedent flow where the same authors noted a 38% reduction in total bedload flux as antecedent duration was increased. Using a unimodal gravel distribution and conditioning flow periods between 1 and 200 minutes Masteller and Finnegan (2017) noted an 86% reduction in bedload flux. This reduction was characterised by a linear reduction in cumulative bedload flux in the period following antecedent flows which was attributed to the re-organisation of the highest protruding grains on the bed surface. However, they note the antecedent durations they used needed to be increased to more accurately constrain the bedload flux relationships with antecedent flow. This link between changes in bedload transport rate and bed topography in response to periods of sub threshold flow was also quantified by Ockelford and Haynes (2012). Using the same distributions and antecedent time periods as reported herein, they quantified changes to bed topography pre and post application of sub threshold flows. They noted that stress history response of the bed surface was grade specific, where bed roughness decreased in uniform beds but increased in graded beds in response to the application of the antecedent flow period. This was reasoned to be due to the uniform bed having larger pore spaces and a greater freedom to rearrange (Ockelford and Haynes, 2012). Grade dependent bed stability, related to both entrainment thresholds and bedload flux, has also been linked to the proportion of fines within a distribution controlling its stability response.

Frostick et al. (1984) suggested that past floods control the proportion of fine sediment infiltrated into the coarser matrix, changing the sediment transport conditions of future floods. Marquis and Roy (2012) noted that bed dilation/contraction caused by fine sediment infiltration or winnowing in a gravel framework related to bed conditions left by previous events, highlighting the role of flood history on sediment transport in gravel-bed rivers.

Research to date has therefore shown that when beds are exposed to periods of antecedent flow they appear to stabilise. This has been shown as both a change to the critical shear stress and the magnitude and timing of bedload flux. However, the differences in the methodologies used, the different timeframes employed and the single grades investigated within the small body of previous stress history literature precludes direct comparison of data. To date no studies have directly compared the response of both entrainment threshold and bedload flux within the same set of experiments and thus it has been difficult to explicitly link one with the other.

This paper is the first to explore the relationship between the evolving critical shear stress and bedload flux characteristics in response to varying inter-flood durations in gravel bed rivers. We present a series of flume experiments that directly compares three sediment grades of equivalent D_{50} and examines their response to changing inter-flood duration. In so doing, we highlight a grade dependent response to inter-flood duration which has implications for the deterministic definition of entrainment and hence accurate prediction of the transition between river bed stability and instability.

2. Methodology

2.1 Experimental Procedure

Experiments were performed within a flow-recirculating, tilting flume (13m long × 1.8m wide × 0.35m deep), set to a bed slope of 1/200. Within the flume, a 2m length of coarse, immobile sediment located immediately downstream of the inlet (to help prevent scour and induce fully turbulent flow) preceded an 8m test length of mobile test sediments that was screeded to a 60mm depth (~4Dmax where Dmax is the maximum grain size of 16mm). Due to the low transport rates within experiments, no notable scour or water surface perturbations were discernible at the immobile-mobile bed transition.

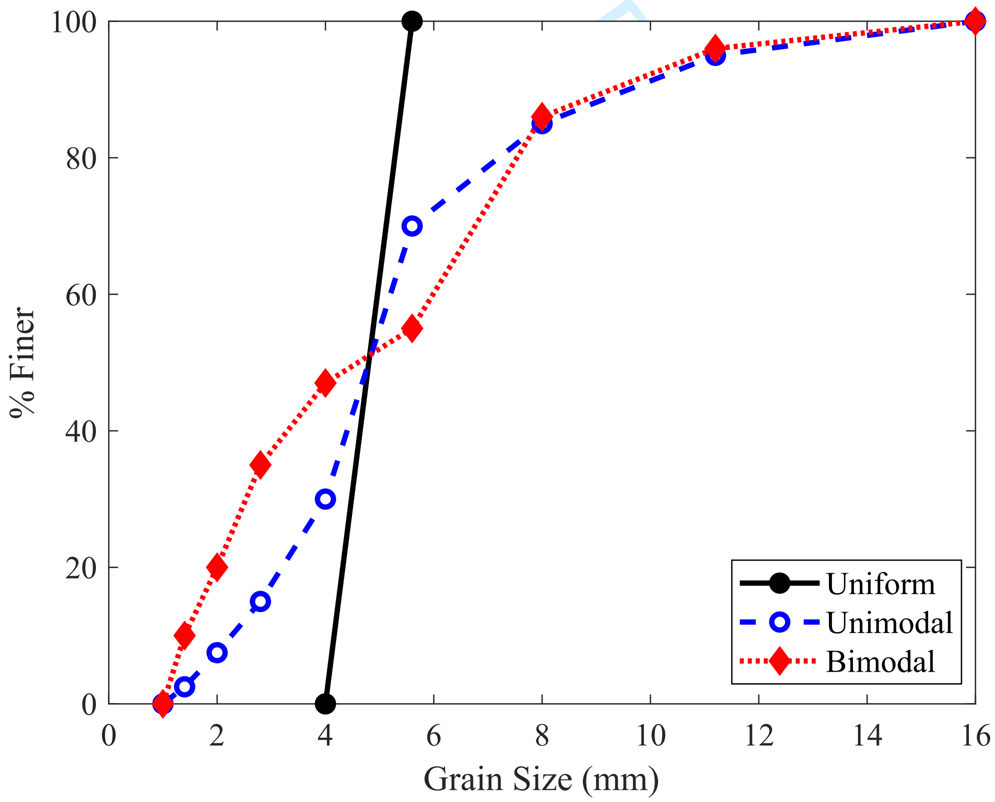

Figure 1: Grain size distribution for the three test sediment grades. The is calculated according to $\sigma_g = (D_{84}/D_{16})^{0.5}$

Three grain size distributions of identical D_{50} (4.8mm); near-uniform (σ_g = 1.13), unimodal (σ_g = 1.63) and bimodal (σ_g = 2.08) were generated using natural sub-rounded sand and gravel ranging from 1 to 16mm in diameter (Krumbein, 1941) with a density of 2560km/m^3 (Figure 1). Sediments were dry sieved to obtain eight size fractions at standard ½ phi intervals and then recombined into the desired distributions with the D_{50} and D_{84} fractions painted for identification purposes (Table 1). During each experiment three phases were run: (a) an initial bedding in period; (b) an antecedent flow period and; (c) a stability test (Figure 2).

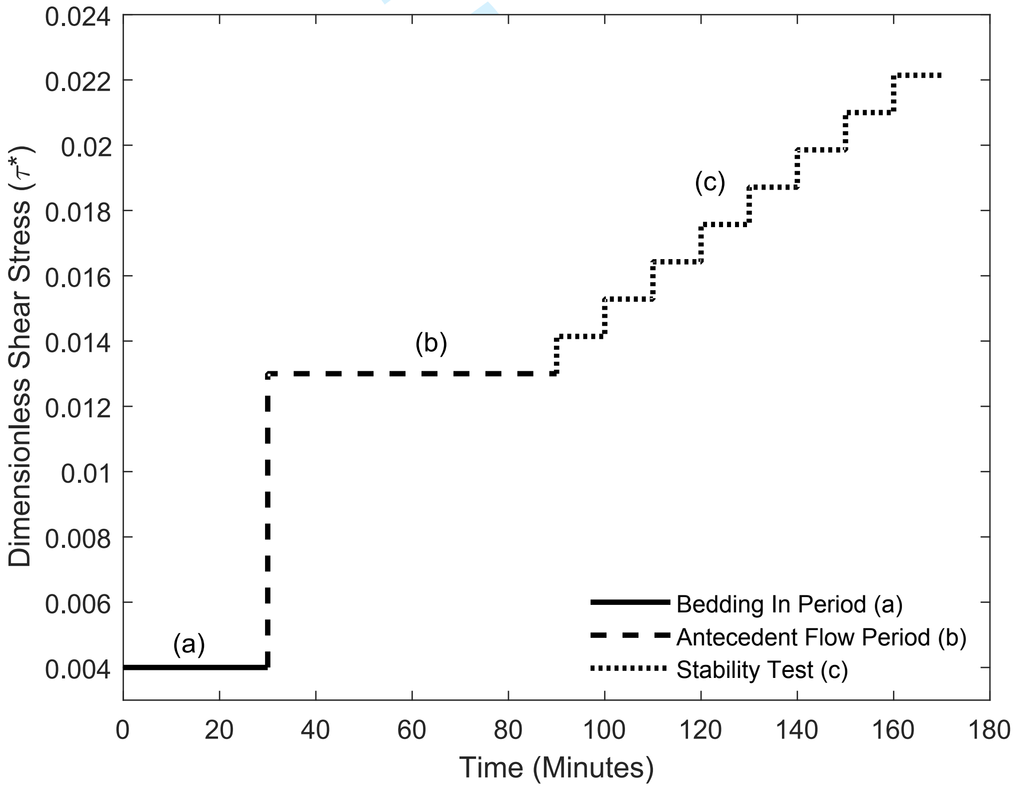

Figure 2: Sample experimental hydrograph detailing the three stages of the experiment: (a) an initial bedding in period run for 30 minutes at $\tau^* \sim 0.004$; (b) an antecedent flow period run at τ^*_{c50} for 0, 60,120, 240 or 960 minutes; and (c) a stability test run until τ^*_{c50} is reached. The dimensionless shear stress values for each phase of each experiment are given in Table 1 with the example here given for the uniform bed exposed to 60 minutes of antecedent flow.

The bedding-in period employed a flow depth of 10 mm ($\tau^* \sim 0.004$) for 30 minutes duration; this was designed to remove any air pockets or unstable grains generated within the bed screeding process. In line with the methodology of Ockelford and Haynes (2012), flow was then increased to apply a shear stress equating to 50% of the critical threshold for entrainment of the median grain size (τ^*_{c50}) benchmarked for when no inter- flood flow was applied (i.e. 0 minutes of antecedent flow applied with τ^*_{c50} values under these conditions given in Table 1). This was calculated using the quantitative visual definition of threshold of Neill and Yalin (1969) in which the number of grain detachments (m_i) from a given bed area (A) over a given time (t) were counted, and the threshold determined according to Equation 1.

$$m_i = \frac{\varepsilon A t}{\sqrt{\frac{\rho D^5}{(\rho_s - \rho) g}}} \qquad \text{(Eq. 1)}$$

where a lower limit of ε was defined by Neill and Yalin as 1.0 x 10^{-6}, and ρ_s and ρ are the sediment and fluid density respectively. The observation area (A) was located in the centre of the flume 11m downstream of the inlet, this was sized 0.04m^2 and the time of observation (t) was set 180 seconds. Once the threshold number of detachments was reached critical shear stress was estimated from the depth-slope product corrected for the roughness effects of both the side walls and the bed according to Manning's *n* and derived according to the methodology followed by Monteith and Pender (2005). This second flow stage constituted the 'antecedent' period, with applied dimensionless shear stress values of 0.016, 0.020, 0.019 of the D_{50} for the uniform, unimodal and bimodal beds respectively. Antecedent flows were applied for either 0 (benchmark), 60, 120, 240 or 960 minutes. No sediment entrainment was observed during this period and quasi-uniform sub-critical flow was maintained throughout.

A final flow stage, the 'stability test' was then applied in steps of increasing shear stress. The shear stress was increased by approximately 0.24 Nm^{-2} during each step which equated to a 5mm flow depth increase or a dimensionless shear stress increase of 0.003 at each step. The stability test was run until the threshold criterion derived from Neill and Yalin were satisfied. Flow steps were 600 second increments which was sufficient to allow flow stabilisation and visual assessment, using the Yalin criterion, of whether or not the new entrainment threshold had been reached. Since the critical shear stress varied according to both grain size distribution and antecedent duration the applied the stability test duration ranged from 50 to 80 minutes (Table 1). Each of these experiments was repeated three times. Reported critical dimensionless shear stress values were calculated from an average of these three experimental runs (first three experiments detailed for each experiment combination in Table 1).

Bedload data was collected from one additional, separate run for each of the experiment combinations (the fourth experiment detailed in Table 1). During this separate experiment, bedload data was collected at each step of the stability test, where each step was 600 seconds long as per the entrainment threshold analysis experiments. Flow was stopped once the critical entrainment threshold, as calculated from the three previous entrainment threshold experiments, was reached. Mobile sediment was collected in a trap located 12m downstream of the flume inlet with sampling slot 75mm wide and of streamwise length 150mm. Bedload was collected at each step of the stability test and collected material was air dried overnight and sieved the individual size fractions. Bedload flux calculations were both integrated over the entire stability test (Figure 4), as well as over the individual steps of the stability test (Figure 5). Fractional transport rates were calculated from the total bedload collected during the final step of the stability test which represents the critical threshold conditions of the D_{50} (Figure 6). Sediment was not recirculated or fed into the flume during the individual experiments but was returned to the flume between experiments. The bed was fully mixed and re-screeded between experiments to preclude inheritance effects from previous experiments. A total of 60 discrete experiments (including repeats) were undertaken (Table 1).

2.2 Experimental Uncertainty

The experiments presented herein allow for the quantification of inter-flood duration effects on bed stability via the direct measurement of critical shear stress and bedload flux. However, methodological issues can introduce uncertainty into these measurements including: (i) inaccurate screeding such that the grain size distribution of the starting bed surface distribution varies between the different experiments; and, (ii) issues of subjectivity surrounding the derivation of threshold according to the Yalin Criterion. Given the D_{50} and D_{84} fractions were coloured, the effects of screeding were analysed using bed surface photographs taken after the initial screed. The numbers of grains belonging to each fraction were counted and the D_{50}:D_{84} ratio calculated. Results indicate ≤1.5% variability between the screeded beds, providing confidence that any differences in bed composition stem solely from the active processes pertaining to the experiment itself. The subjectivity in use of the Yalin Criterion was minimised via data collection using a single operator. Comparison of multiple repeats of runs shows an average variability of 4.8% in terms of the calculated average critical dimensionless shear stress (Table 1; this is in line with experimental error of similar laboratory studies (Piedra and Haynes, 2011). The highest variability is typically associated with the shortest antecedent flow durations where there is the greatest rate of change in the shear stress. As such the variability in the average critical shear stress is never larger than the absolute change in shear stress and does not therefore change the relationship between critical shear stress and antecedent duration.

3. RESULTS

3.1 Inter-flood duration effects on entrainment threshold

The relationship between entrainment threshold and inter-flood duration is summarised by Figure 3. Under benchmark conditions with no inter-flood flow applied critical dimensionless shear stress shows a hierarchy to bed stability: unimodal (0.039): bimodal (0.033); uniform (0.031). After the application of the antecedent period there is a positive correlation with between the antecedent duration and dimensionless critical shear stress for all three grain size distributions. However, the magnitude of the increase in critical shear stress compared to the benchmark experiments is grade specific: near uniform (+18%) > bimodal (+12%)> unimodal (+9%).

There is also an apparent difference between the rate of change in critical dimensionless shear stress in response to the applied antecedent flow. In order to quantify the rate of change, parametric curves have been applied to the entrainment threshold data. The fitted curves used herein are distinct from the only other previous attempt to model growth of Paphitis and Collins (2005) whose 'exposure correction' described logarithmic growth of their entrainment threshold function in response to increasing inter-flood durations. Whilst their mathematical form correctly describes progressive slowing of growth of inter-flood duration effects over lengthening timeframes, it holds an implicit assumption of unbounded growth as time tends towards infinity; i.e. if left for a prolonged period of time, the bed will keep gaining in stability. As a sediment bed cannot become infinitely stressed, such a logarithmic description is inaccurate; rather, it must tend to a limiting value commensurate with the stability maxima of the bed. Two alternative mathematical forms are, therefore, considered which both start and tend to finite values. Such parametric curves have been used in ecological modelling (Noy-Meir,1978) and in enzyme kinetics (Michaelis and Menten, 1913) to describe similar rates of change characterised by an initially linear increases which slows asymptotically towards some maximal value. The first is described by Equation 2 below with the fit parameters given in Table 2.

$$\tau_c = \tau_{\max} - (\tau_{\max} - \tau_0)e^{-kt} \qquad \text{(Eq. 2)}$$

where τ_c represents the critical dimensionless shear stress, *t* represents antecedent duration (minutes), $\tau_{\max}$ is the maximal critical dimensionless shear stress, τ_0 gives the initial critical dimensionless shear stress and *k* is a free parameter (units $mins^{-1}$) controlling how quickly τ_c increases. This model assumes that there is a maximum possible stress and that the difference between the current stress and the maximum stress decreases exponentially.

The alternative model is described by Equation 3 with the fit parameters given in Table 3:

$$\tau_c = \tau_0 + t\left(\frac{\tau_{\max} - \tau_0}{t + t_{1/2}}\right) \qquad \text{(Eq. 3)}$$

where τ_c represents the critical dimensionless shear stress, t represents antecedent duration (minutes), $\tau_{\max}$ is the maximal critical dimensionless shear stress, τ_0 gives the initial critical dimensionless shear stress and $t_{1/2}$ is the time until half the maximal shear stress has been reached (minutes). Thus, both Eq. 2 and Eq. 3 assume than when $t = 0$ then $\tau_c = \tau_0$; when $t \rightarrow \infty$ then $\tau_c \rightarrow \tau_{max}$. The best fit models were selected based on minimising the squared error between the model and the observed data points.

The R^2, RSME and SSE data are similar for both model fits and describe the data well (Tables 2 and 3); the fits derived from Equation 2 are shown in Figure 3 given the greater model skill and are described below. As reported, the parametric curve indicates the uniform bed to be the most responsive to the effects of antecedent flow duration and the unimodal the least (Figure 3, Table 2). The model indicates that the rate of increase in critical dimensionless shear stress in response to increased inter-flood duration varies between distributions as indicated by the time to half-life. The unimodal bed has the greatest rate of response to inter-flood flows where the time to half-life occurs within 74 minutes. This is compared to the bimodal and uniform beds which take approximately twice and three times as long respectively. However, both models predict that if antecedent duration continues to increase there will be very little further stability gains; there will be a further percentage increase in stability of 5%, 2% and 1% for the uniform, unimodal and bimodal beds respectively.

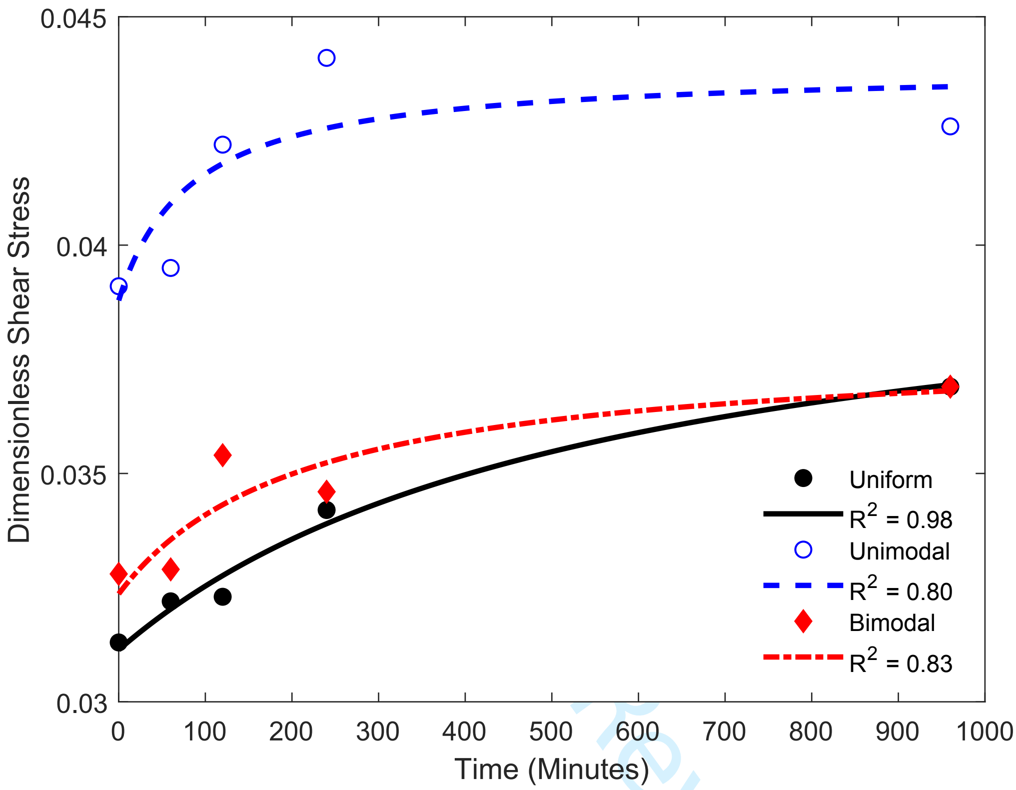

Figure 3: The relationship between antecedent duration, average critical dimensionless shear stress and grain size distribution with fits plotted derived according to Equation 2.

3.2 Inter-flood duration effects on bedload transport rate and characteristics

Both the magnitude and rate of response to the applied antecedent flow is grade dependent. Given most sediment transport formulae rely on the use of a single critical value of shear stress (e.g., Meyer-Peter and Müller, 1948; Engelund and Fredsøe 1975; Wong and Parker, 2006) understanding how periods of prolonged, inter-flood flow affect the onset of motion could be used to reduce the uncertainty in these. Previous research has linked changes to entrainment thresholds in response to periods of sub threshold flow with changes to the magnitude and rate of bedload flux (Haynes and Pender, 2007; Masteller and Finnegan, 2017). As such, transport rate and fractional analysis of the bedload transported during the stability test was undertaken to provide insight into the links between changes to entrainment thresholds and the subsequent bedload flux characteristics.

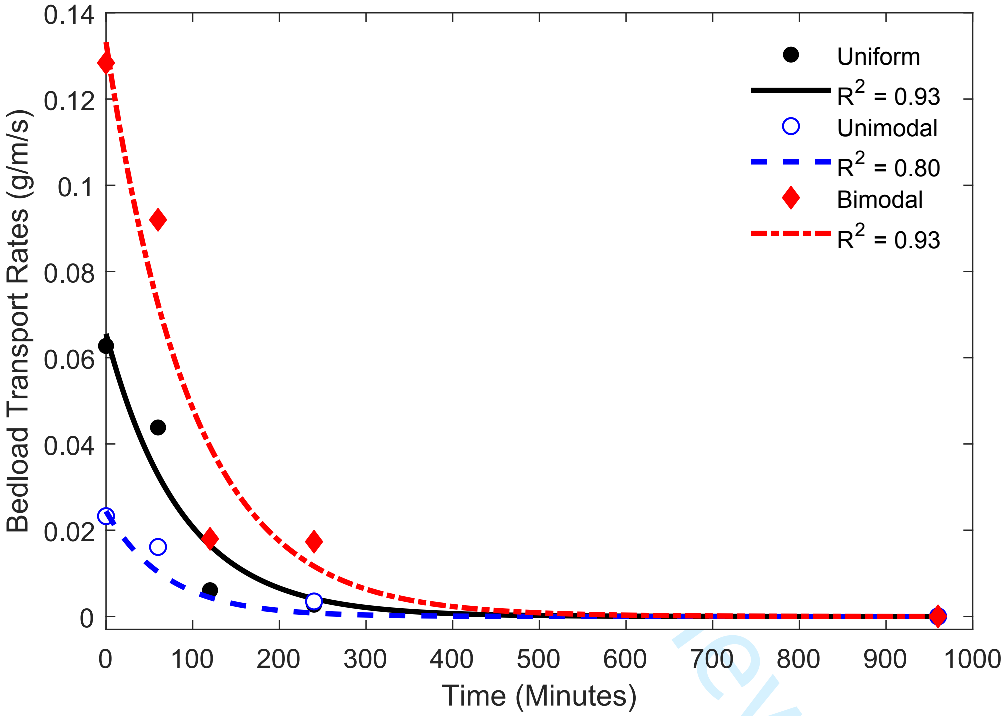

Figure 4: Inter-flood duration relationships with bedload transport rate, including the fitted exponential decay function of form $\Sigma Q_{bi} = \Sigma Q_{bi0} + (\Sigma Q_{bi\infty} - \Sigma Q_{bi0})e^{-kt}$ with R^2 values of 0.93, 0.80 and 0.93 for the uniform, unimodal and bimodal beds respectively.

Following 960 minutes of antecedent conditioning, bedload transport rates were reduced by 91% for bimodal beds, 80% for near uniform beds, and 60% for unimodal beds (Figure 4, Table 4). The relationship between antecedent duration and bedload transport rate can be described by an exponential decay, however, akin to the entrainment threshold data, the rate of change is grade sensitive as indicated by the half life value. The unimodal bed has the most rapid rate of decline with a half-life time of approximately 48 minutes compared to the uniform and bimodal beds which have half live times of 60 and 68 minutes respectively. Further, data indicates that rate of reduction is linked with the predicted minimal transport rate value derived in Table 4. Specifically, the unimodal bed decays the fastest but has a higher overall predicted minimal transport rate as compared to the bimodal bed which decays over the longest time period but decays to a lower minimal transport rate, as given in Table 4.

In addition to reported relationships between inter-flood duration and bedload flux, previous data has indicated that prolonged periods of sub threshold flow also have the potential to delay to the onset of entrainment in the following flood (Reid and Frostick, 1984). The first three subplots of Figure 5 plot $\frac{\tau^*}{\tau_c^*}$ at each step of the stability test as a function of the bedload transport rate for the same step of the stability test. The fitted trend line given in each of the subplots combines all of the date for each bed and collapses them onto a single straight line using a least-square error fitting approach; the power law fitted follows that of previous studies (Parker, 1990; Wilcock and Crowe, 2003; Recking 2010; Piedra, 2010) applicable to ranges of $\frac{\tau^*}{\tau_c^*}$ < 1.3. The final subplot of Figure 5 directly compares the trend lines derived for each sediment bed.

For all three grain size distributions, there is the expected positive correlation between dimensionless shear stress and total load such that increased time into the stability test is correlated with an increase in transported load for each step of the stability test. An inverse relationship is also noted between the antecedent duration and transported load in each step of the stability test whereby a decrease in total load is correlated to an increase in antecedent duration. Finally, there is an offset noted on the abscissa in the two graded beds such that transport does not commence until later in the stability test (i.e. at higher shear stresses) as antecedent duration is increased; this is particularly noted within the bimodal bed. This suggests that the mechanisms responsible for stabilising the bed are different between the uniform and graded beds.

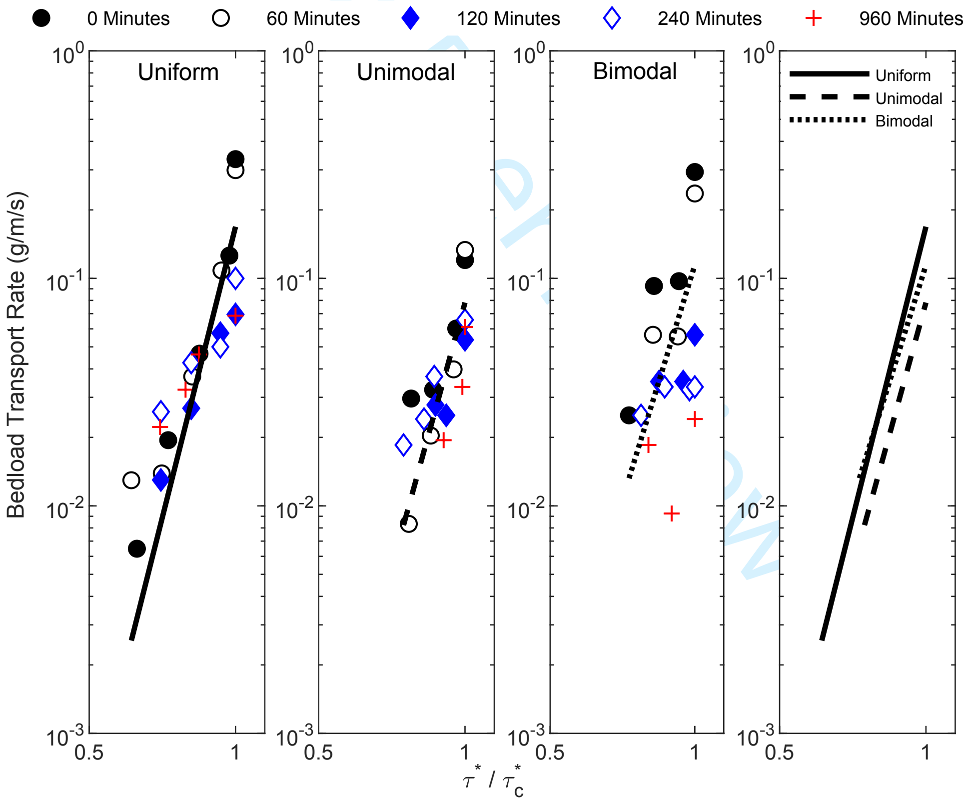

Figure 5: Relationship between $\frac{\tau^*}{\tau_c^*}$ at each step of the stability test as a function of the bedload transport rate for the same step of the stability test for the uniform, unimodal and bimodal beds respectively (subplots 1-3). The fitted trend line given in each of the subplots combines all of the date for each bed and collapses them onto a single straight line. The final subplot directly compares the trend lines derived for each sediment bed. The exponent of the power law relationship is 11.06, 10.09 and 8.77 and the R_2 values of those fits are 0.63, 0.75 and 0.29 for the uniform, unimodal and bimodal beds respectively.

When the data is scaled in terms of excess shear stress ($\frac{\tau^*}{\tau_c^*}$), the data appear to collapse onto a single relationship. However, it is also clear that whilst the data seems to more readily collapse for the uniform and unimodal beds the bimodal bed exhibits significant scatter and the data derived from the longest inter-flood durations (240 and 960 minutes) is not described well by the trend line.

Given the different rate and magnitude of response of the graded beds to increasing inter-flood durations the following section uses fractional bedload transport patterns to analyse the stability-mobility patterns of individual fractions within each bed in order elucidate upon the underpinning bed stabilisation processes (Figure 6). Given that the stability test was curtailed at the threshold for D_{50}, if size selective entrainment is prominent no grains greater than the D_{50} should be moving ($g_i/F_i \neq 1$); however, if grains greater than the D_{50} are moving then there is a tendency towards equal mobility conditions ($g_i/F_i = 1$).

The unimodal bed is characterised by equal mobility conditions under 0 and 60 minutes of antecedent flow. However as antecedent duration is increased beyond that the bedload response becomes more strongly size selective in the coarse and fine end members of the distribution such that these grains stabilise and leave the middle fractions of the transported distribution as being comparatively mobile. In comparison, under benchmark conditions, the bimodal bed is characterised by equal mobility particularly for in the grain fractions containing and surrounding the median grain size. As antecedent duration is increased although size selective transport conditions begin to develop in the finest members of distribution the degree of size selectivity which develops is not as strong as that which develops in the unimodal bed.

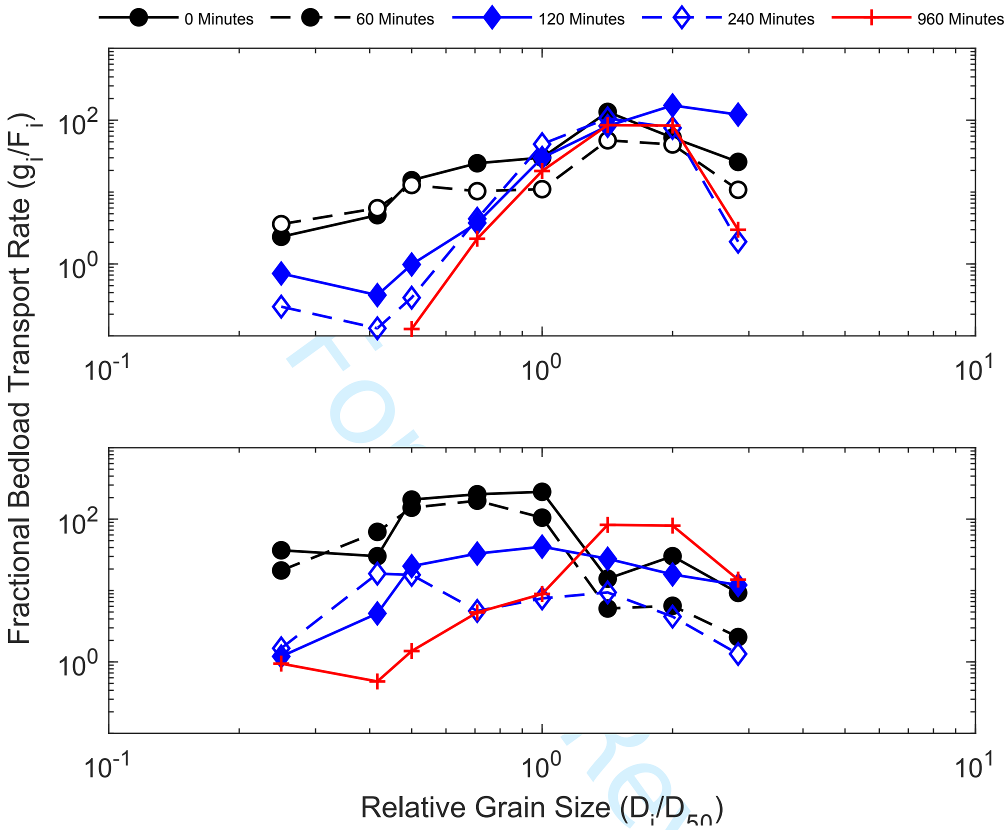

Figure 6: Fractional bedload transport rate of the unimodal (top plot) and bimodal bed (bottom plot) scaled by the abundance of each size (gi) in the bulk mix (Fi) plotted against dimensionless grain size for antecedent durations 0-960mins. Given the stability test was stopped once the critical entrainment threshold of the D_{50} had been reached the data in this figure represent bedload which was collected during the last step of the stability test under these conditions.

4. DISCUSSION

4.1 Effect of inter-flood duration on bed stability

This paper has provided the first direct quantification of the response of different grain size distributions to inter-flood duration effects in terms of both entrainment threshold and bedload flux response. Analysis shows that all three grain size distributions responded to changes in antecedent duration. This is supportive of field (e.g. Reid and Frostick, 1984; Reid *et al*., 1985; Willetts *et al*., 1987; Oldmeadow and Church, 2006; Pfeiffer and Finnegan, 2018) and laboratory (Paphitis and Collins, 2005; Monteith and Pender, 2005; Haynes and Pender, 2007; Masteller and Finnegan, 2016) data which have both indirectly and directly suggested that antecedency may be an important control on entrainment thresholds and bedload flux.

Critical shear stress of the median grain size increases by up to +18% after being exposed 960 minutes of antecedent flow, with the uniform grain size distribution being the most responsive and the unimodal least responsive. The changes to entrainment threshold in this study are under half that noted by Paphitis and Collins (2005) and Haynes and Pender (2007) who observed up to a 56% and 46% increase in critical bed shear stress respectively. The sediment beds reported by Paphitis and Collins (2005) were finer (0.19 to 0.77mm sand) and there were differences in the bed preparation techniques between studies which is likely to explain the differences in the observed results; screeded beds (this study; Church, 1978; Cooper and Tait, 2008) form more resistant initial structures than those formed under still water conditions (Paphitis and Colins, 2005). Although Haynes and Pender (2007) used the same bimodal mixture as this current paper the timescales were significantly longer than those reported herein and they also used a discharge was above-threshold for the D_{50}.

The changes to entrainment threshold have been linked with bed reorganisation during the sub threshold flow period (Hassan and Church, 2000; Haynes and Pender, 2007; Ockelford and Haynes, 2012; Masteller and Finnegan, 2016). Given that the applied antecedent flow in this paper was set at τ^*_{c50}, active, large scale processes of reorganisation as a result of grain entrainment are unlikely and thus significant bed surface composition change should not occur (Sutherland, 1991; Hassan and Church, 2000; Whiting and King, 2003). Instead inter-flood processes appear to increase the importance of passive, grain scale processes which, in turn, alter a beds resistance to entrainment via a change to surface texture (Dietrich *et al*., 1989; Kirchner et al., 1990; Fenton and Abbott, 1997; Schmeeckle and Nelson, 2003; Ockelford and Haynes, 2012). Specifically, Masteller and Finnegan (2016) observe that the largest change in the bed surface elevation distribution occurs in the tails of the distribution and this change is positively correlated to antecedent flow duration. They attribute this to pivoting of unstable grains into more stable positions, the filling of pockets left by displaced grains and the oscillation, reorientation and reduced relative protrusion of grains which occur throughout the antecedent flow period.

Results from this paper have also shown that grain size distribution is a key control on the magnitude of response to inter-flood duration in terms of entrainment threshold response; direct comparison shows uniform beds to be up to twice as responsive as graded beds. Ockelford and Haynes, (2012) suggest the differences in response between the uniform and graded beds is related to changes in bed roughness which develop during the antecedent period. Using bed surface topography data collected pre and post antecedent flows they observed a 12% decrease in roughness of uniform beds as compared to a 15% and 40% increase in roughness of unimodal and bimodal beds respectively. In the uniform bed the decrease in bed roughness reduced the relative depth of localised pores and hence reduced both the shear stress magnitude and variability across the bed surface (Li and Komar, 1986; Kirchner *et al.,* 1990; Rollinson, 2006). Within the graded beds, the magnitude of the inter-flood flow response is controlled by the rearrangement of the bed which is permitted due the range of grain sizes. During the sub threshold flows vertical winnowing of the finer grains serves to consolidate the framework gravels and hence increase bed stability (Frostick *et al*., 1984; Reid *et al*., 1985; Carling *et al*., 1992; Allan and Frostick, 1999; Marion *et al*., 2003; Ockelford and Haynes, 2012).

However, data in this paper also indicates that the degree of response to increasing inter-flood duration in graded beds is strongly linked to the percentage of fines in the distribution such that the bimodal bed, which has the highest proportion of fines (20% of the distribution between 1-2mm compared to 7.5% in the unimodal bed) responds to a greater degree than the unimodal bed. It is thought that the process of consolidation of the beds due to the infiltration of fines as described above drives this response. This is in agreement with Cooper *et al*., (2009), who assessed the resistance to bedload transport of unimodal and bimodal deposits of similar D_{50} by linking stability with the organisation of the surface deposits. Initially, their bimodal beds had a higher degree of mobility due to a higher proportion of the fluid force being carried by the finer grain fractions. However, as flow periods were increased, a higher proportion of the fluid force was carried by the larger grains due to grain sheltering (Schmeeckle and Nelson, 2003) and the development of grain structures (Hassan and Church, 2000), such that the differences in the stability of the two beds decreased.

The greatest rate of change in critical shear occurs for the shortest antecedent durations which is in line with previous stress history research Paphitis and Collins, 2005; Monteith and Pender, 2005; Haynes and Pender, 2007; Ockelford and Haynes 2012; Masteller and Finnegan, 2016. However, interestingly the rate of change is also grade specific where the unimodal bed responds to increasing inter-flood flow duration is 2.5 times faster than the bimodal bed and 3 times as fast as the uniform bed. Given the applied antecedent shear stress is set at τ^*_{c50} , it seems logical that the uniform bed is less mobile under antecedent flows hence, it will take longer to respond but once the bed has reorganised it will not be able to rearrange any further. Within the graded beds the rearrangement processes responsible for stabilising the bed will occur rapidly during the onset of the higher discharge conditions experienced during the antecedent flow period but once the fines have winnowed through the surface and consolidated the bed very little further rearrangement will occur (Ockelford and Haynes 2012).

In relation to the bedload response to inter-flood duration up to a 91% reduction in the bedload transport rate after 960 minutes of applied antecedent flow is observed. Akin to the response of critical shear stress, the reduction in bedload transport rate with increasing antecedent duration is nonlinear. This agrees with the previous results of Haynes and Pender (2007) who also note an exponential decline in transport rates as antecedent duration is increased. Whilst Masteller and Finnegan (2016) fitted a linear model to their cumulative bedload flux data as a function of increased conditioning flow, they do state that an exponential decline function also fitted their data, albeit with lower model skill. Thus, these results are consistent with an overall reduction in grain mobility, implying an increase in critical Shield's stress with increased conditioning time. Such behaviour is similar to that of many degradation experiments (Tait *et al.,* 1992; Proffitt and Sutherland, 1983; Pender *et al*., 2001). Haynes and Pender (2007) attributed this decay to the progressive stabilisation of larger areas of the bed surface such that grains became unavailable for transport. The decay to a constant flux even under the low shear stresses is possible due to turbulent fluctuations in the flow (e.g. Grass, 1970; Paintal, 1971; Graf and Pazis, 1977; Lavelle and Mofjeld, 1987; McEwan *et al*.,2004; Paphitis and Collins, 2005; Bottacin *et al.,* 2008) or to the fact that a population of high protruding grains is always available for transport (Masteller and Finnegan, 2016).

There is an observable delay to the onset of entrainment in periods of unsteady flow subsequent to sub threshold flow periods. During floods a hysteresis loops often develop in sediment flux measurements, whereby different magnitudes of bedload flux are produced on the rising and falling limbs of hydrographs for the same flow magnitude (Reid *et al*., 1985; Church *et al*., 1998; Hassan *et al*., 2006; Waters and Curran, 2015; Mao, 2018). These studies have proved an intrinsic link between bed structure characteristics and the total load transported (Reid *et al*., 1985; Reid *et al*., 1997), which serve to alter entrainment thresholds and hence bedload flux. Although this paper has not run a full hydrograph after the sub threshold flow period, the theoretical underpinnings behind the links between stability, surface structure and sediment flux are transferable. This is evidenced by the fact that not only does the data in this paper show a an offset in the initiation of motion, but that the total loads are also be reduced for comparable shear stresses of the unsteady flow as sub threshold flow duration is increased.

Although the bedload flux data appears to collapse readily for the uniform and unimodal beds the bedload transport rates associated with the longest inter-flood durations in the bimodal bed are not well described. This is supported by Piedra (2010) who analysed five commonly employed sediment transport equations and found that the rapid increase in transport rates with shear stress for approximately $\frac{\tau^*}{\tau_c^*}$ < 1.3 and the drastic reduction of the rate of increase of sediment transport rate at $\frac{\tau^*}{\tau_c^*}$ > 1.3 (Wiberg and Smith, 1989 Hassan and Woodsmith, 2004; Bathurst, 2007) did not explain the relationships shown when sediment beds had been exposed to prolonged periods of antecedent flow. Piedra related the deviation caused by the effects of antecedent duration, as shown by the data herein, to stabilisation of the bed surface and the delay to the onset of entrainment caused by bed surface rearrangement. Neither factor are taken into account in commonly used transport equations which derive critical entrainment thresholds purely based on bed grain size distribution data and bed slope (Reid and Frostick, 1986; Gomez and Church, 1989; Wong 2003; Recking, 2010).

A change in the fractional transport rates following the antecedent conditioning phase is reported. Typically, fractional bedload rates would tend towards moving from size selective transport patterns under low shear stress, partial transport conditions to equal mobility conditions under high shear stress, full mobility conditions (Wilcock and McArdell, 1997; Shvidchenko and Pender, 2000). Since the stability test in this paper was run until τ^*_{c50} it is assumed that the fractional mobility patterns would be characterised by size selective entrainment owing to the partial mobility conditions. This would be irrespective of the preceding applied antecedent duration. In the unimodal bed there is a trend towards equal mobility in the intermediary size fractions with selective entrainment of the end members of the distribution (Ashworth and Ferguson, 1989; Wilcock and Southard, 1988; Kuhnle, 1992; Wilcock and McArdell, 1993; Laronne *et al.*, 1994). However as antecedent duration is increased the bedload response becomes more strongly size selective in the coarse and fine end members of the distribution; as this typically goes hand-in-hand with an increase in grain hiding the effect is on mobility of the middle fractions of the transported distribution (Brayshaw *et al.,*1983; Li and Komar, 1986; Dietrich *et al.*, 1989; Fenton and Abbott, 1997). Conversely in the bimodal bed, under benchmark conditions, the bimodal bed is characterised by equal mobility particularly for in the grain fractions containing and surrounding the median grain size. As antecedent duration is increased, size selectivity begins to develop, particularly in the finest members of distribution which appear to have stabilised on the bed surface. This leaves the coarsest fractions to be over represented in the bedload. This suggests that there are significant hiding effects which develop in response to increasing inter-flood durations and underpin the theory that it is the relative size effects which drive the response to inter-flood duration (Jackson and Beschta, 1984; Ikeda and Iseya, 1988; Wilcock, 1988).

4.2 Implications

A number of important implications for river flows emerge from our results. Increased bed stability in response to increased inter-flood duration manifests itself via increased critical shear stress which may preclude reliable estimates of bedload transport, as most predictive models reply on a specified critical shear stress (e.g., Meyer-Peter and Müller, 1948; Engelund and Fredsøe 1975; Wong and Parker, 2006). Despite numerous revisions to the Sheild’s function, a single value of flow intensity at particle entrainment is not just a disputed concept (Lavelle and Mofjeld, 1987) but its value has been shown to depend on a range of particle parameters such as shape, size distribution and armouring (Parker et al., 1982; Carsons and Griffiths, 1985; Carling et al., 1992; Buffington and Montgomery, 1997; Church et al., 1998). These observations of an evolving, or history-dependent critical shear stress which is related to grain size distribution makes the transition towards gravel bed instability and active sediment transport difficult to predict and could form the basis for incorporating an inter flood-duration 'correction factor' into existing entrainment equations.

In order to correct for the effects of inter-flood flows entrainment thresholds need to be based on experimental data derived from beds which have been exposed to antecedent flows. The relationship between bedload transport rate and excess shear stress used herein can be described by a power law similar with similar exponent values to that used by previous authors (Parker, 1990; Wilcock and Crowe, 2003; Recking 2010; Piedra, 2011). However, as supported by Piedra (2011) data in this paper also indicates that there is no unique equation with fixed parameters capable of describing bedload transport behaviour for gravel channels which have been exposed to differing inter-flood flow periods. Further, given changes in bed stability in response to inter-flood flow duration are grade sensitive our results indicate the not only is predicting entrainment based on a single critical Shields value inaccurate but also that the D_{50} may not be the best grain fraction from which to estimate entrainment thresholds (MacKenzie et al, 2018). This study has shown that the finest and coarsest fractions are most responsive to inter-flood flow duration and hence more realistic entrainment models might consider using these fractions to define bed stability (Carling, 1987,1988; Ashworth and Ferguson,1989; Eaton and Church, 2004; Tamminga et al., 2015; Eaton et al., 2015; MacKenzie and Eaton, 2017).

Increased pressure on water resources will require sophisticated environmental flow guidelines to maintain habitat diversity, ensure ecosystem health and functioning, and enable effective water resource management planning (Poff et al., 1997; Tharme, 2003; 2010; Rolls & Arthington, 2014). Given managed flows are designed to mimic natural flow regime and sediment dynamics, periods of prolonged low flow prior to release will have a fundamentally different sediment transport response than those with shorter low flow periods. Hence this research has significant implications for the management and design of such flows (Lytle & Poff, 2004; Arthington et al., 2006; Kiernan et al., 2012; Olden & Naiman, 2010; Poff and Schmidt, 2016).

5. CONCLUSION

Novel laboratory experiments in a recirculating flume have quantified the effects between grain size distribution and inter-flood duration on gravel river bed stability. Inter-flood duration effects have been shown to be ubiquitous regardless of surface grain size distribution where direct entrainment threshold analysis shows that critical shear stress of the median grain size increases by up +18% due to the applied inter-flood duration of 960 minutes at τ^*_{c50}. The magnitude of response is contingent upon grain size distribution; uniform beds are more responsive as compared to the graded beds. The effects of inter-flood duration on entrainment thresholds can be well predicted using models which both start and tend to finite values such that when t = 0 then $\tau_c = \tau_0$; when $t \to \infty$ then $\tau_c \to \tau_{max}$. Bedload transport rate has also been shown to be responsive to inter-flood duration where up to a 91% reduction in bedload was recorded for the longest antecedent flow periods. However, akin to the entrainment threshold data there is also a grade dependent response which has been attributed to the ability of the bed to rearrange into a more stable configuration during the sub threshold flow periods. Changes in the transport pattern reflect this stabilisation process where the percentage of fines within a distribution control the extent to which equal mobility or size selective conditions are noted.

Results have implications for the prediction of entrainment thresholds, the accurate prediction of bedload flux timing and magnitude and have implications for the management of environmental flow design. However questions still remain as to how antecedent shear stress magnitude may affect the stability gains and whether there may be a threshold at which inter-flood flows may serve to destabilise the bed surface. Further, an understanding of the interaction of the bed surface with the overlying fluid flow regime with respect to the changes in the turbulent patterns during inter-flood sub-threshold flows would also be a significant step forward in this emerging research field.

Acknowledgements

This research was funded by the Engineering and Physical Sciences Research council (EPSRC) under grant code EP/EO30467/1 *held by Haynes. The work was undertaken at the School of Engineering, University of Glasgow and the authors sincerely thank the technical staff for their assistance in this research. The authors* *would like to thank the detailed reviewers comments received on the first draft of this paper which have strengthened the paper greatly.*

References

Allan, A.F. and Frostick, L.E. 1999. Framework dilation, winnowing and matrix particle size: the behaviour of some sand-gravel mixtures in a laboratory flume. Journal of Sedimentary Research 69: 21–26

Arthington, A., Bunn, S., Poff, N., & Naiman, R. 2006. The Challenge of Providing Environmental Flow Rules to Sustain River Ecosystems. Ecological Applications 16; 1311-1318.

Ashmore, P. 1988. Bedload transport in braided gravel-bed stream models. Earth Surface Processes and Forms 13: 677-695.

Ashworth PJ, Ferguson RI. 1989. Size-selective entrainment of bed-load in gravel bed streams. Water Resources Research 25: 627–634.

Bagnold, R. A. 1980. An empirical correlation of bedload transport rates in flumes and natural rivers. Proceedings of the Royal Society of London Series A 372; 453-473.

Barry, J. J., Buffington, J. M., Goodwin, P., King, J. G., and Emmett, W. W. 2008. Performance of bed-load transport equations relative to geomorphic significance: predicting effective discharge and its transport rate. Journal of Hydraulic Engineering 13: 601-615.

Bathurst, J.C. (2007). Effect of coarse surface layer on bedload transport. Journal of Hydraulic Engineering 133: 1192-1205.

Bottacin-Busolin, A., Tait, S.J., Marion, A., Chegini, A., and Tregnaghi, M. 2008. Probabilistic description of grain resistance from simultaneous flow field and grain motion measurements. Water Resources Research. doi; 0.1090.2007WR006224

Buffington, J.M. and Montgomery, D.R. 1997. A systematic analysis of eight decades of incipient motion studies, with special reference to gravel-bedded rivers. Water Resources Research. 33; 1993–2029.

Carling P. 1987. Bed stability in gravel streams, with reference to stream regulation and ecology. In River Channels: Environmental and Process, Richards K (eds), Institute of British Geographers Special Publications Series, Wiley-Blackwell: Oxford; 321–347

Carling P. 1988. The concept of dominant discharge applied to two gravel-bed streams in relation to channel stability thresholds. Earth Surface Processes and Landforms 13: 355–367

Carling, P. A., A. Kelsey, and Glaister, M.S. 1992. Effect of bed roughness, particle shape and orientation on initial motion criteria. In Dynamics of Gravel-bed Rivers. Billi, P., Hey, R.D., Thorne, C.R. and Tacconi, P, (eds). Wiley; Chichester: 24–39

Carson, M.A. and Griffiths, G.A. 1987. Bedload Transport on gravel channels. Journal of Hydrology 79; 375-378

Church, M. 1978. Palaeohydraulic Reconstructions From a Holocene Valley Fill. In: Fluvial Sedimentology; Miall, A.D. (eds). Canadian Society of Petroleum Geologists. Calgary. Canada. 743–772.

Church, M., Hassan, M.A. and Wolcott, J.F. 1998. Stabilizing self organized structures in gravel-bed stream channels: Field and experimental observations. Water Resources Research 34; 3169-3179.

Cooper, J.R. and Tait, S.J. 2008. Water worked gravel beds in laboratory flumes- a natural analogue?. Earth Surface Processes and Landforms 34: 384-397.

Cooper, J.R. and Frostick, L.E. 2009. The difference in the evolution of the bed surface topography of gravel and gravel-sand mixtures, 33rd IAHR Congress: Water Engineering for a Sustainable Environment. International Association of Hydraulic Engineering & Research. Vancouver, Canada.

Dietrich, W.E., Kirchner, J.W., Ikeda, H. and Iseya, F. 1989. Sediment supply and the development of the coarse surface layer in gravel-bedded rivers. Nature 340; 215-217

Eaton, B.C. Church, M. 2004. A graded stream response relation for bed load-dominated streams. Journal of Geophysical Research 109: F03011. doi.org/10.1029/2003JF000062

Eaton B, MacKenzie, L., Jakob, M. and Weatherly, H. 2017. Assessing erosion hazards due to floods on fans: Physical modelling and application to engineering challenges. Journal of Hydraulic Engineering 143: 04017021. doi.org10.1061/(ASCE)HY.1943-7900.0001318

Engelund, F. And Fredsoe, J. 1976. A sediment transport model for straight alluvial channels. Hydrology Research 7:293-306. doi.org/10.2166/nh.1976.0019

Fenton, J. D. and Abbott, J. E. 1977. Initial movement of grains on a stream bed: the effect of relative protrusion. Proceedings of the Royal Society of London. 352; 523–537

Frostick, L.E., Lucas, P.M. and Reid, I. 1984. The infiltration of fines into coarse-grained alluvial sediments and its implications for stratigraphical interpretation. Journal of the Geological Society of London. 141; 955-965.

Gomez, B. 1983. Temporal variations in the particle size distribution of the surficial bed material: the effect of progressive armouring. Geografiska Annaler. 65; 183-192.

Gomez, B. And Church, M. 1989. An assessment of bed load sediment transport formulae for gravel bed rivers. Earth Surface Processes and Landforms 25: 1116-1186. doi.org/10.1029/WR025i006p01161

Graf, W.H. and Pazis, G.C. 1977. Deposition and erosion in an alluvial channel. Journal of Hydraulic Research. 15; 151-166.

Grass, A.J. 1970. Initial instability of fine bed sand. Journal of the Hydraulics Division; American Society of Civil Engineering. 96; 619-632

Hassan, M.A. and Church, M. 2000. Experiments on surface structure and partial sediment transport on a gravel bed. Water Resources Research. 36; 1885-1895.

Hassan, M. A. and Woodsmith, R. D. 2004. Bed load transport in an obstruction-formed pool in a forest, gravel bed stream. Geomorphology 58: 2003-221.

Hassan, M.A., Egozi, R., Parker, G., 2006. Experiments on the effect of hydrograph characteristics on vertical grain sorting in gravel bed rivers. Water Resources Research. doi.org/10.1029/2005WR004707.

Haynes, H. and Pender, G. 2007. Stress history effects on graded bed stability. Journal of Hydraulic Engineering 33; 343-349.

Kiernan, J., Moyle, P. and Crain, P.K. 2012. Restoring native fish assemblages to a regulated California stream using the natural flow regime concept. Ecological Applications. 22: 1472-1482

Kirchner, J.W., Dietrich, W.W., Iseya, F. and Ikeda, H. 1990. The variability of critical shear stress, friction angle, and grain protrusion in water-worked sediments. Sedimentology 37; 647–672.

Krumbein, W. C. 1941. Measurement and geological significance of shape and roundness of sedimentary particles. Journal of Sedimentary Petrology 1; 64-72.

Lavelle, W. and Mofjeld, H. O. 1987. Do critical stresses for incipient motion and erosion really exist? Journal of Hydraulic Engineering 113: 370-388.

Li, Z. and Komar, P.D. 1986. Laboratory measurements of pivoting angles for applications in selective entrainment of gravel in a current. Sedimentology 33; 5917-5929.

Lytle, D.A. and Poff, N. 2004. Adaption to natural flow regimes. Trends in Ecology and Evolution. 2: 94-100

MacKenzie, L.G., Eaton, B.C. and Church, M. 2018. Breaking from the average: Why large grains matters in gravel bed streams. Earth Surface Processes and Landforms DOI: 10.1002/esp.4465

MacKenzie LG, Eaton BC. 2017. Large grains matter: Contrasting bed stability and morphodynamics during two nearly identical experiments. Earth Surface Processes and Landforms 42: 1287–1295

Mao, L. 2018. The effects of flood history on sediment transport in gravel bed rivers. Geomorphology. 322: 192 – 205.doi.org/10.1016/j.geomorph.2018.08.046

Marquis, G.A., Roy, A.G., 2012. Using multiple bed load measurements: toward the identification of bed dilation and contraction in gravel-bed rivers. Journal of Geophysical Research. 117, F01014. doi.org/10.1029/2011JF002120

Masteller, C.C. and Finnegan, N.J. 2017. Interplay between grain protrusion and sediment entrainment in an experimental flume. Journal of Geophysical Research: Earth Surface 122: 274-289 doi.org/10.1002/2017GL076747

Masteller, C.C., Finnegan, N.J., Turowski, J.M., Yager, E.M. and Rickermann, D. 2019. History dependent threshold for motion revealed by continuous bedload transport measurements in a steep mountain stream. Geophysical Research Letters 46; 2583-2591

Marion, A., Tait, S.J. and McEwan, I.K. 2003. Analysis of small-scale gravel bed topography during armouring. Water Resources Research 39; 1334-1345.

McEwen, I.K., Sorensen, M., Heald, J., Tait, S.J., Cunningham, G.J., Goring, D.G. and Willetts, B.B. 2004. Probabilistic modeling of bed-load composition. Journal of Hydraulic Engineering. 130; 129-139.

Meyer-Peter, E. and Müller, R. 1948. Formulas for bedload transport. Proceedings of the 2nd Meeting of the International Association for Hydraulic Research, 3: 39–64.

Monteith, H. and Pender, G. 2005 Flume investigation into the influence of shear stress history. Water Resources Research 41, doi:10.1029/2005WR004297.

Neill, C.R. and Yalin, M.S. 1969. Quantitative definition of bed movement. Journal of the Hydraulics Division, American Society of Civil Engineers 95; 581-588.

Ockelford, A. And Haynes, H. 2012. The impact of stress history on bed structure. Earth Surface Processes and Landforms DOI: 10.1002/esp.3348

Olden, J.D. and Naiman, R.J. 2009. Incorporating thermal regimes into environmental flows assessments: modifying dam operations to restore freshwater integrity. Freshwater Biology. 55: 86-107

Oldmeadow, D.F. and Church, M. 2006. A field experiment on streambed stabilization by gravel structures. Geomorphology 78; 335–350.

Paintal, A.S. 1971. A stochastic model for bed load transport. Journal of Hydraulic Research. 9; 527–553.

Paphitis, D. and Collins, M.B. 2005. Sand grain threshold, in relation to bed stress history: an experimental study. Sedimentology 52; 827 838.

Parker, G. 1990. Surface-based bedload transport relation for gravel bed rivers. Journal of Hydraulic Research 28: 417-436.

Parker, G., Dhamotharan, S., Stefan, H. 1982. Model experiments on mobile, paved gravel bed streams. Water Resources Research18: 1395-1408.

Pender, G., Hoey, T.B., Fuller, C. and Mcewan, I.K. 2001. Selective bedload transport during the degradation of a well sorted graded sediment bed. Journal of Hydraulic Research 39; 269-277.

Pfeiffer, A.M. and Finnegan, N.J. 2018. Regional variation in gravel riverbed mobility, controlled by hydrologic regime and sediment supply. Geophysical Research Letters 45: 3097- 3106 doi.org/10.1002/2017GL076747

Piedra, M., (2010). Flume investigation of the effects of sub-threshold rising flows on the entrainment of gravel beds. Unpublished Ph.D. Thesis. Department of Civil Engineering. The University of Glasgow

Piedra, M. and Haynes, H. 2011. The spatial distribution of coarse surface grains and the stability of gravel river beds. Sedimentology 59 (3); 1014-1029

Poff, N. L. and Schmidt, J. 2016. How dams can go with the flow. Science. 353:1099- 1100. DOI: 10.1126/science.aah4926

Poff, N.L., J.D. Allan, M.B. Bain, J.R. Karr, K.L. Prestegaard, B.D. Richter, R.E. Sparks, and J.C. Stromberg. 1997. The natural flow regime: a paradigm for river conservation and restoration. BioScience 47:769-784.

Powell, D. M., Reid, I. and Laronne, J. B. 1999. Hydraulic interpretation of cross-stream variations in bed-load transport. Journal of Hydraulic Engineering125; 1243-1252.

Powell, D. M., Reid, I. and Laronne, J. B. 2001. Evolution of bedload grain size distribution with increasing flow strength and the effect of flow duration on the caliber of bed load sediment yield in ephimeral gravel bed rivers. Water Resources Research 37: 1463-1474.

Proffitt, G. T., and Sutherland, A. J. 1983. Transport of non uniform sediments. Journal of Hydraulic Research 21; 33–43.

Recking, A. 2010. A comparison between flume and field bed load transport data and consequences for surface-based bed load transport prediction. Water Resources Research doi:10.1029/2009WR008007.

Recking, A., Liebault, F., Peteuil, C. and Joliment, T. 2012. Testing bedload transport equations with consideration of time scales. Earth Surface Processes and Landforms. 37: 774-789 doi.org/10.1002/esp.3213

Reid, I. and Frostick, L.E. 1984. Particle interaction and its effects on the thresholds of initial and final bedload motion in coarse alluvial channels. Sedimentology of Gravels and Conglomerates. In Koster, E.H and Steel, R.J.S. (eds). Canadian Society of Petroleum Geologists Memoir. 10: 61-68.

Reid, I., Frostick, L.E. and Layman, J.T. 1985. The incidence and nature of bedload transport during flood flows in coarse-grained alluvial channels. Earth Surface Processes and Landforms 10: 33-44.

Rollinson, G.K. 2006. Bed structure, pore spaces and turbulent flow over gravel beds. Unpublished Ph.D. Thesis. Department of Civil Engineering. The University of Hull.

Schmeeckle, M.W. and Nelson, J.M. 2003. Direct numerical simulation of bedload transport using a local, dynamic boundary condition. Sedimentology 50; 279-301.

Scheider, J., Rickermann, D., Turowski, J. and Kirchner, J. W. 2015. Self-adjustment of stream bed roughness and flow velocity in a steep mountain channel. Water Resources Resarch. 51: 7838-7859 doi.org/10.1002/esp.3213

Rolls, R,J, and Arthington, A,H. 2014. How do low magnitudes of hydrologic alteration impact riverine fish populations and assemblage characteristics? Ecological Indicators. 39:179–88.

Shaw, J. and Kellerhals, R. 1982. The composition of recent alluvial gravels in Alberta River beds. Alberta Research Council Bulletin 41; 151.

Shvidchenko, A.B., and Pender, G. 2000 Flume study of the effect of relative depth on the incipient motion of coarse uniform sediments. Water Resources Research. 36: 619 -628.

Sutherland, A. 1991. Hiding functions to predict self armouring. Proceedings, International Grain Sorting Seminar. ETH Zürich. 117; 273-298.

Tait, S.J., Willetts, B.B. and Maizels, J.K. 1992. Laboratory observations of bed armouring and changes in bedload composition. In Dynamics of Gravel-bed Rivers. Billi, P., Hey, R.D., Thorne, C.R. and Tacconi, P. (eds). Wiley; Chichester. 205-225.

Tamminga AD, Eaton BC, Hugenholtz CH. 2015. UAS-Based remote sensing of fluvial change following an extreme flood event. Earth Surface Processes and Landforms 40(11): 1464–1476.

Tharme, R.E. 2003. A global perspective on environmental flow assessment: emerging trends in the development and application of environmental flow methodologies for rivers. River Research and Applications 19: 397-442.

Waters, K.A., Curran, J.C., 2015. Linking bed morphology changes of two sediment mixtures to sediment transport predictions in unsteady flows. Water Resoures Research. 51: 2724–2741. https://doi.org/10.1002/2014WR016083.

Whiting, P. and King, J. 2003. Surface particle sizes on armoured gravel streambeds: Effects of supply and hydraulics. Earth Surface Processes and Landforms 28:1459–1471.

Wiberg, P. L. and Smith, J. D. 1989. Model for calculating bedload transport of sediment. Journal of Hydraulic Engineering 1: 101-123.

Wilcock, P.R. 1993. Critical shear stress of natural sediments. Journal of Hydraulic Engineering. 119: 491-505.

Wilcock, P. R. and Crowe, J. C. 2003. Surface-based transport model for mixed-size sediment. Journal of Hydraulic Engineering 129: 120-128.

Wilcock, P. R. and McArdell, B.W. 1997. Partial transport of a sand/gravel sediment. Water Resources Research 33; 235-245.

Willetts, B.B., Maizels, J.K. and Florence, J. 1987. The simulation of stream bed armouring and its consequences. Proceedings of the Institute of Civil Engineering. 1; 799-814.

Wong, M. and Parker, G. 2006. Reanalysis and correction of bedload relation of MeyerPeter and Müller using their own database. Journal of Hydraulic Engineering 132:1159–1168.

Zhang, X. and McConnachie, G. L. 1994. A reappraisal of the Engelud bed load equation. Hydrological Sciences Journal 39; 561-567.

Experiment Number	Distribution	Antecedent Flow Duration (Minutes)	Stability Test Duration (Minutes)	Critical Flow Depth (m)	Recorded Critical Dimensionless Shear Stress values	Average Critical Dimensionless Shear Stress
1,2,3,4	Near - Uniform	0	70	0.051 (0.025)	0.021, 0.019, 0.019	0.020 (0.013)
5,6,7,9		60	70	0.052	0.021, 0.02, 0.022	0.021
9,10,11,12		120	70	0.052	0.023, 0.021, 0.022	0.022
1314,15,16		240	80	0.056	0.022, 0.021, 0.023	0.022
17,18,19,20		960	90	0.060	0.025, 0.022, 0.024	0.024
21,22,23,24	Unimodal	0	80	0.063 (0.032)	0.026, 0.024, 0.024	0.025 (0.010)
25,26,27,28		60	80	0.064	0.026, 0.025, 0.025	0.026
29,30,31,32		120	90	0.069	0.028, 0.027, 0.026	0.027
33,34,35,36		240	100	0.072	0.029, 0.028, 0.030	0.029
37,38,39,40		960	90	0.070	0.030, 0.029, 0.029	0.029
41,42,43,44	Bimodal	0	60	0.053 (0.030)	0.022, 0.019, 0.021	0.021 (0.012)
45,46,47,48		60	60	0.054	0.021, 0.02, 0.022	0.021
49,50,51,52		120	70	0.057	0.025, 0.021, 0.024	0.023
53,54,55,56		240	70	0.056	0.024, 0.022, 0.02	0.022
57,58,59,60		960	80	0.060	0.024, 0.025, 0.024	0.024

Table 1; Experimental information for all experiments detailing the length of the antecedent flow, the stability test duration, the critical flow depths and the recorded dimensionless shear stress values at the critical entrainment threshold for all experiments. Values in brackets for the critical flow depth represents the depth at $T^*c_{50\ i.e}$ i.e. the flow depth which was applied during the antecedent flow period. Values in brackets for the average critical dimensionless shear stress represent the T^*c_{50} values under benchmark conditions i.e. the shear stress which was applied during all of the antecedent flow periods calculated from where no antecedent flow is applied.

Bed Fit Parameters	Uniform	Unimodal	Bimodal
Maximal dimensionless shear stress	0.038	0.043	0.037
k (Minutes^{-1})	0.003	0.010	0.004
Time to half saturation (Minutes)	234	74	198
R^2	0.98	0.80	0.83
RMSE	0.0003	0.0013	0.0007
SSE	1.71e-07	1.59e-06	8.84e-07
% increase in dimensionless shear stress between 0-960 minutes	18	9	12
Predicted % increase in dimensionless shear stress between 0- and Max predicted	19	11	13

Table 2; The parameters associated with the growth in shear stress over time according Equation 2

Bed Fit Parameters	Uniform	Unimodal	Bimodal
Maximal dimensionless shear stress	0.040	0.044	0.037
Half Saturation Constant (Minutes)	285	84	214
R^2	0.98	0.71	0.82
RMSE	0.0004	0.0017	0.0011
SSE	5.15E-07	2.27E-06	9.54E-07
% increase in dimensionless shear stress between 0-960 minutes	18	9	12
Predicted % increase in dimensionless shear stress between 0 and Max predicted	24	11	13

Table 3; The parameters associated with the growth in shear stress over time according Equation 3.

Bed Fit Parameters	Uniform	Unimodal	Bimodal
Minimal Bedload Transport rate (g/m/s)	0.015	0.018	0.012
k (Minutes^{-1})	0.0115	0.0143	0.0102
Half Life (Minutes)	60.22	48.37	68.29
R^2	0.93	0.80	0.93
RMSE	0.009	0.006	0.017
SSE	2.38e-04	1.04e-04	8.96e-04

Table 4; The parameters associated with the decay in bedload transport over time according to an exponential decay function

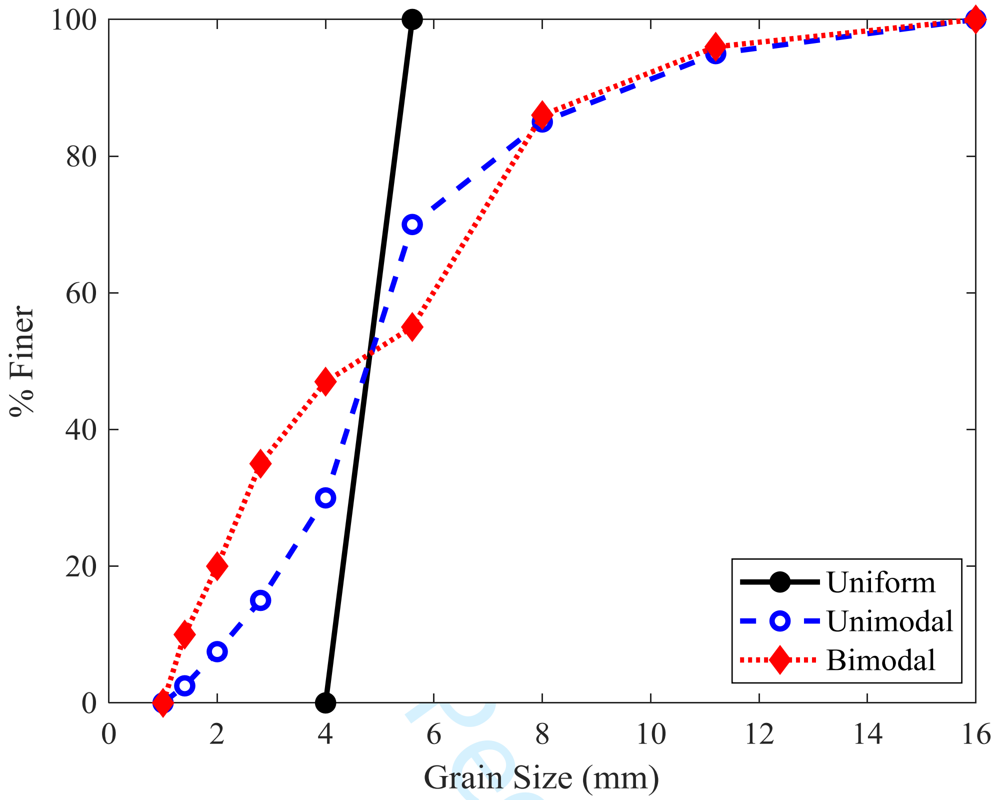

Figure 1: Grain size distribution for the three test sediment grades. The is calculated according to $\sigma_g = \left(D_{84}/D_{16}\right)^{0.5}$

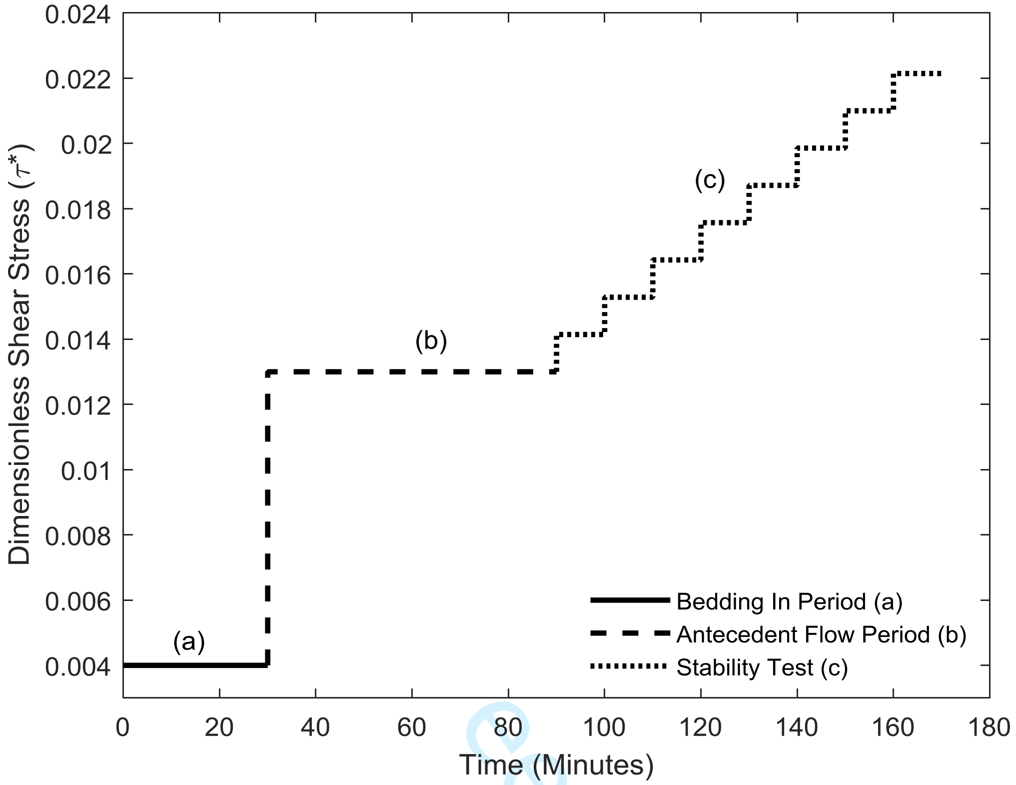

Figure 2: Sample experimental hydrograph detailing the three stages of the experiment: (a) an initial bedding in period run for 30 minutes at $\tau^* \sim 0.004$; (b) an antecedent flow period run at τ^*_{c50} for 0, 60,120, 240 or 960 minutes; and (c) a stability test run until τ^*_{c50} is reached. The dimensionless shear stress values for each phase of each experiment are given in Table 1 with the example here given for the uniform bed exposed to 60 minutes of antecedent flow.

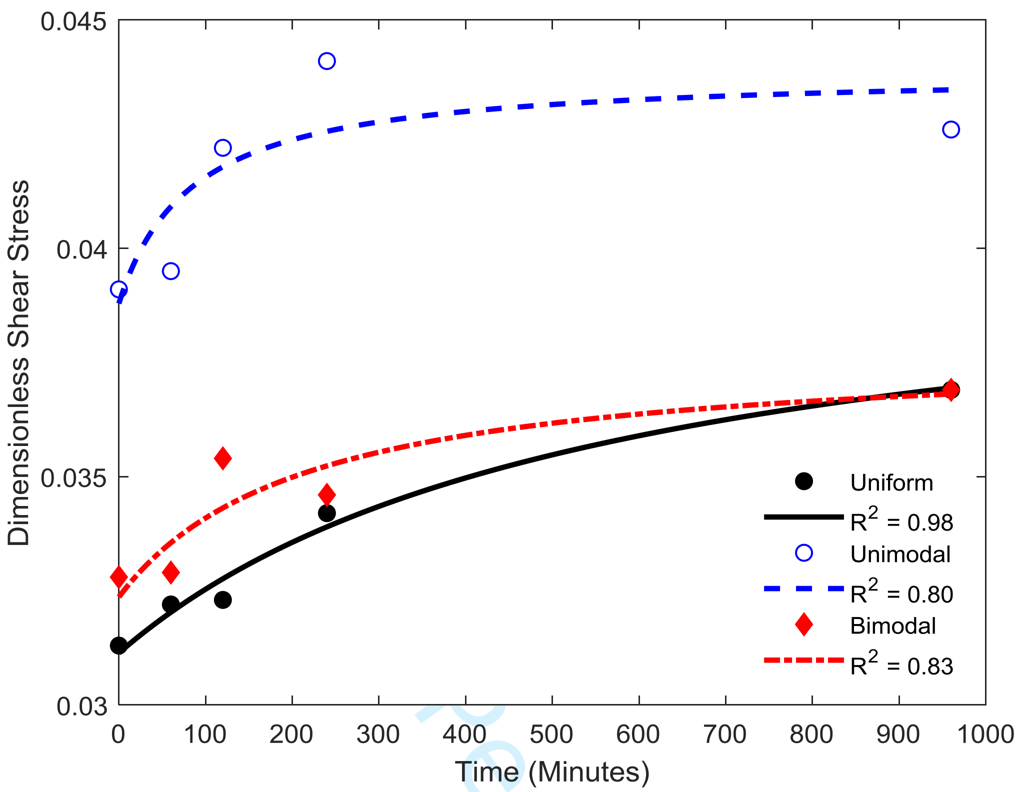

Figure 3: The relationship between antecedent duration, average critical dimensionless shear stress and grain size distribution with fits plotted derived according to Equation 2.

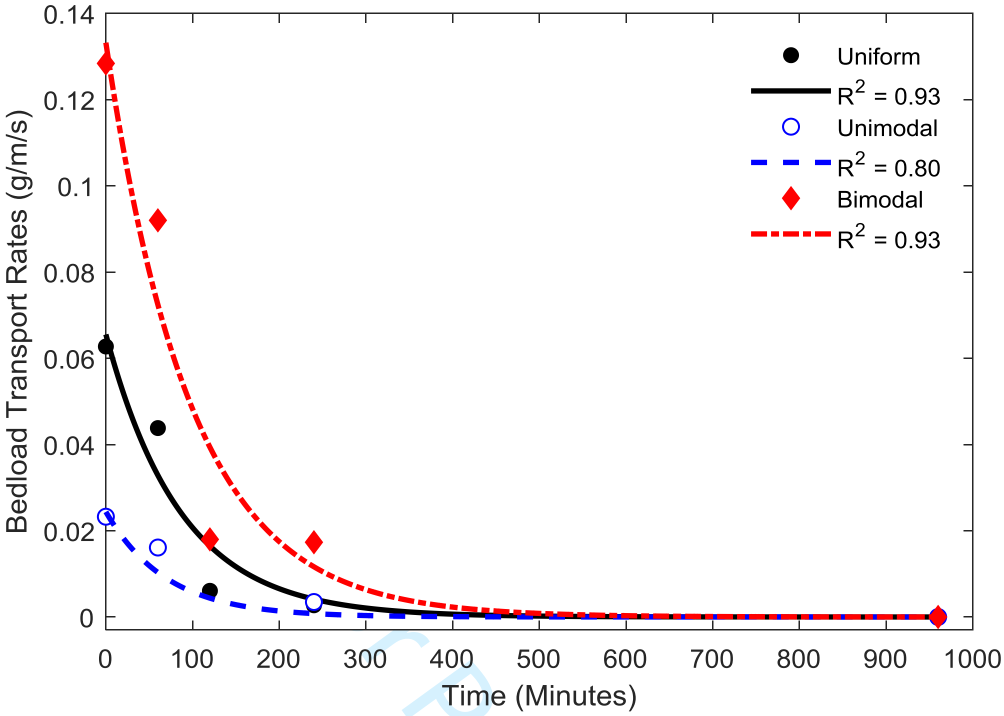

Figure 4: Inter-flood duration relationships with bedload transport rate, including the fitted exponential decay function of form $\Sigma Q_{bi} = \Sigma Q_{bi0} + (\Sigma Q_{bi\infty} - \Sigma Q_{bi0})e^{-kt}$ with R^2 values of 0.93, 0.80 and 0.93 for the uniform, unimodal and bimodal beds respectively.

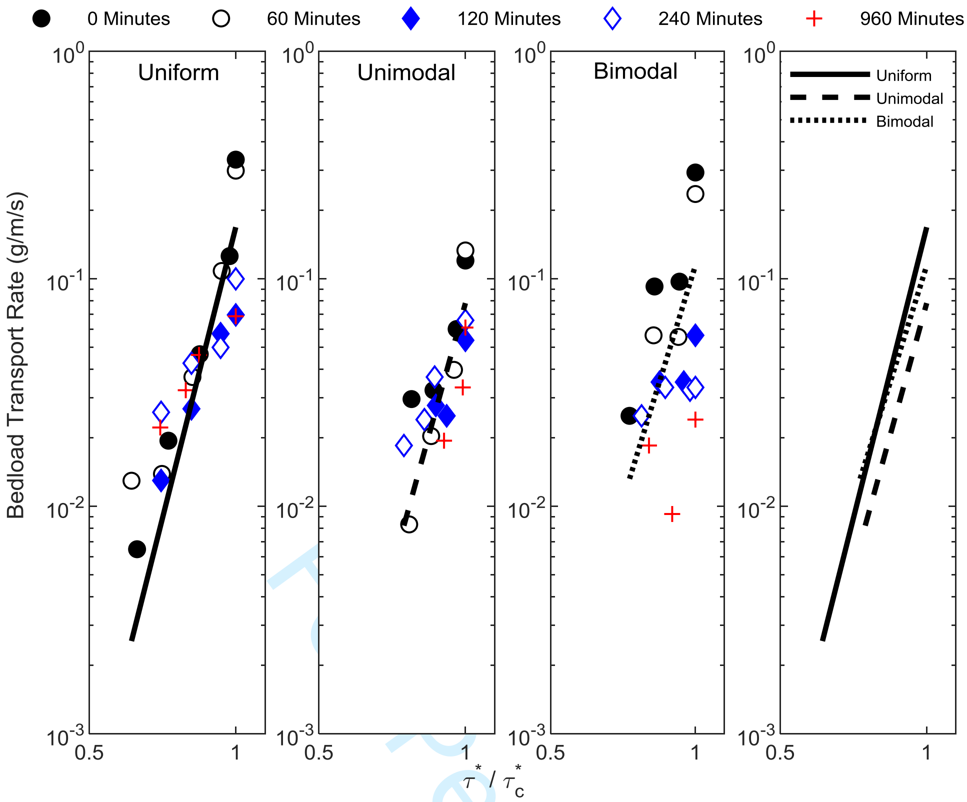

Figure 5: Relationship between $\frac{\tau^*}{\tau_c^*}$ at each step of the stability test as a function of the bedload transport rate for the same step of the stability test for the uniform, unimodal and bimodal beds respectively (subplots 1-3). The fitted trend line given in each of the subplots combines all of the date for each bed and collapses them onto a single straight line. The final subplot directly compares the trend lines derived for each sediment bed. The exponent of the power law relationship is 11.06, 10.09 and 8.77 and the R2 values of those fits are 0.63, 0.75 and 0.29 for the uniform, unimodal and bimodal beds respectively.

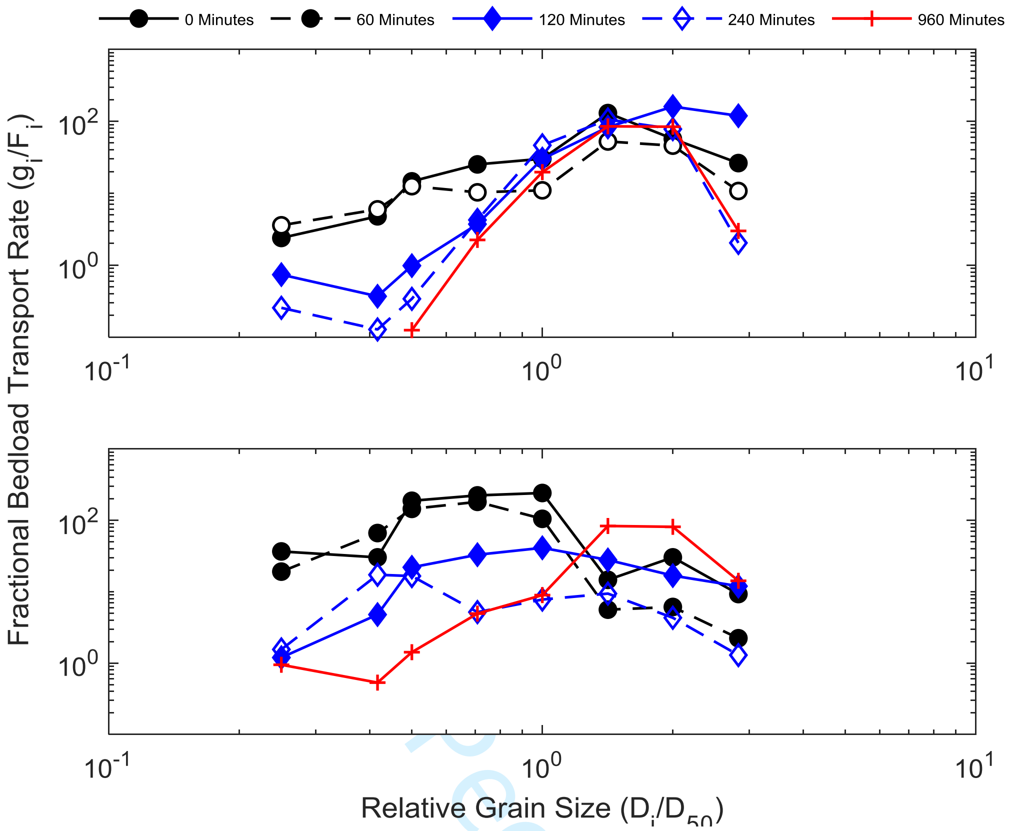

Figure 6: Fractional bedload transport rate of the unimodal (top plot) and bimodal bed (bottom plot) scaled by the abundance of each size (gi) in the bulk mix (Fi) plotted against dimensionless grain size for antecedent durations 0-960mins. Given the stability test was stopped once the critical entrainment threshold of the D_{50} had been reached the data in this figure represent bedload which was collected during the last step of the stability test under these conditions.